

THE IMPACT OF THE SAHARAN AIR LAYER ON ATLANTIC TROPICAL CYCLONE ACTIVITY

BY JASON P. DUNION AND CHRISTOPHER S. VELDEN

The Saharan Air Layer may be yet another piece of the puzzle in advancing our understanding of tropical cyclone intensity change in the North Atlantic and Caribbean.

The Saharan air layer (SAL), an elevated layer of Saharan air and mineral dust, has been investigated for several decades, but its link to Atlantic tropical cyclone (TC) activity has never been fully examined. This work discusses recently developed Geostationary Operational Environmental Satellite (GOES) split-window satellite imagery that permits continuous tracking of the SAL across the North Atlantic, Caribbean, and Gulf of Mexico. This new type of satellite imagery reveals that the SAL may play a major role in suppressing TC activity in the North Atlantic. This paper presents documentation of these suppressing characteristics for a number of specific TC-SAL interactions that have occurred during several recent Atlantic hurricane seasons.

AFFILIATIONS: DUNION—CIMAS, University of Miami, and NOAA/AOML/Hurricane Research Division, Miami, Florida; VELDEN—CIMSS, University of Wisconsin—Madison, Madison, Wisconsin

CORRESPONDING AUTHOR: Jason P. Dunion, NOAA/AOML/Hurricane Research Division, 4301 Rickenbacker Causeway, Miami, FL 33149

E-mail: jason.dunion@noaa.gov

DOI: [10.1175/BAMS-85-3-353](https://doi.org/10.1175/BAMS-85-3-353)

In final form 17 October 2003
©2004 American Meteorological Society

The SAL occurs during the late spring through early fall over extensive portions of the North Atlantic Ocean between the Sahara Desert, the West Indies (Prospero and Carlson 1972), and the United States (as documented by recent GOES satellite imagery). Carlson and Prospero (1972) proposed that a dry, well-mixed layer often extends to ~500 hPa over Africa during the summer months. As this air mass advances westward from the North African coast, often in association with African easterly waves (AEWs; Burpee 1972), it is undercut by cool, moist low-level marine air and becomes the SAL. Just offshore, the SAL's base is at ~900–1800 m and the top is usually below 5500 m (Diaz et al. 1976). Near its southern boundary, the SAL is also associated with the midlevel African easterly jet centered near 700 hPa, which can greatly increase the low-level vertical wind shear. The SAL appears to retain its Saharan characteristics of warm, stable air near its base, and dryness and dustiness throughout its depth as it is carried as far as the western Caribbean Sea (~7000 km from the northwest African coast). Previous work has suggested that the SAL is typically confined to an east–west wavelength of 2000–3000 km (Karyampudi and Carlson 1988). However, the SAL-tracking GOES imagery indicates that the SAL's wavelength can extend to 4000–5000 km and cover an area of the Atlantic slightly larger than the 48 contiguous United States.

Geostationary satellites reveal that the SAL often enhances convection along its western and southern boundaries (Chen 1985), but in its interior, the combination of embedded dry, stable air and strong easterly wind shear inhibits the occurrence of the deep convection that is essential for TC formation. During an average summer, about six named TCs form in the main development region (Goldenberg and Shapiro 1996) of the tropical Atlantic between 10° and 20°N, near the SAL's southern boundary. The GOES SAL-tracking imagery indicates that when both TCs and AEWs [the precursors for ~65% of Atlantic named TCs (Pasch et al. 1998)] are engulfed by the SAL, much of their deep convection dissipates. Consequently, these tropical circulations can lose a major portion of their strength while still over the warm tropical Atlantic.

A METHOD FOR TRACKING THE SAL WITH GOES SATELLITE IMAGERY. The SAL is not readily detectable with the individual visible and infrared (IR) channels on the GOES imager. Although visible satellite imagery can detect the SAL's suspended mineral dust in the eastern North Atlantic, the dust becomes more diffuse and difficult to monitor as the air in the SAL moves westward. Because of the SAL's limited vertical extent (~500–850 hPa), the dry air it contains can be difficult to detect with traditional water vapor imagery available from the 6.5- and 6.7- μm channels on the GOES satellites. These channels respond most sensitively to radiation emitted at approximately 400 hPa (Velden et al. 1998). Therefore, dry SAL air below ~500 hPa may be undetectable when the air above the SAL is relatively moist. Although the individual spectral channels on the GOES satellites were not designed to track the SAL, recent tests have shown that the position of the SAL's dust and lower-tropospheric dry air can be tracked most reliably with the split-window IR channels (10.7 and 12 μm) on the GOES-8 imager (Prata 1989). These IR channels are unlike the water vapor channels because they have weighting functions in the lower troposphere. The SAL signal they detect is not affected by variations in upper-level moisture (in cloud-free areas).

The mineral dust and dry lower-tropospheric air in the SAL reduce the brightness temperature differences that typically exist between the 10.7- and 12- μm channels on GOES-8. These changes in brightness temperature differences allow the SAL to be tracked over time and space. Under typical cloud-free atmospheric conditions, the 10.7- μm IR emissions originate closer to the earth's surface than do those in the 12- μm IR channel, which is more sensitive to absorption by low-level water vapor. Because the 10.7- μm channel more effectively senses the near-surface atmosphere, its signal is usually warmer than the 12- μm channel. However, the SAL environment affects the 12- μm signal in two ways. First, the exceptionally dry air in the SAL results in a decrease in the amount of IR absorption by low-level moisture, thus, increasing the brightness temperatures in the 12- μm channel. This acts to reduce the brightness temperature difference between the 10.7- and 12- μm channels. Second, suspended mineral dust in the SAL absorbs some of the incident solar radiation it receives and reradiates it as longwave IR radiation. Dust emits this radiation more effectively at 12 μm than at 10.7 μm . Therefore, the dust further reduces the brightness temperature difference between the 10.7- and 12- μm channels and, in extreme dust events, can even reverse the sign of the difference. Image enhancements were developed to take advantage of these temperature anomalies measured by the GOES IR channels to track the SAL. Typical brightness temperature (BT) differences between the 12- and 10.7- μm channels ($\text{BT}_{12} - \text{BT}_{10.7}$) in the non-SAL tropical Atlantic range from +5° to 10°C. Brightness temperature differences between –4° and +4°C are enhanced to track the SAL in the GOES-8 imagery. The ability of this satellite imagery to detect the SAL air mass was verified using moisture information from Global Positioning System (GPS) dropwindsondes (GPS sondes; Hock and Franklin 1999) and is discussed in the section titled “dry air intrusion into the TC circulation.”

In early 2003, GOES-8 was replaced by GOES-12. This new satellite does not have a 12- μm channel. Therefore, a similar SAL-tracking algorithm was developed for GOES-12 that substitutes the 10.7- and 12- μm channels with 3.9- and 10.7- μm channels, respectively. The brightness temperature differences between the 10.7- and 3.9- μm channels ($\text{BT}_{10.7} - \text{BT}_{3.9}$) in the non-SAL tropical Atlantic typically range from +6° to 10°C. The GOES-12 algorithm applies the same principles previously discussed for the GOES-8 technique to track the dry, dusty air in the SAL. This slightly modified algorithm enhances brightness temperature differences ($\text{BT}_{10.7} - \text{BT}_{3.9}$) between –13° and +5°C to identify the SAL, and was calibrated using the original methods and imagery developed with GOES-8. However, because of solar contamination inherent with the 3.9- μm channel, this new algorithm is only useful for tracking the SAL during nighttime hours.

CHARACTERISTICS OF THE SAL AFFECTING TC FORMATION. Enhanced low-level temperature inversion. The temperature at the base of the

SAL (~800–900 hPa) is often 5°–10°C warmer than the Jordan (1958) mean tropical sounding (Diaz et al. 1976). While the warmth of the air above the SAL's base results from its origin over the Sahara, it is maintained by the absorption of solar radiation by the suspended mineral dust. This daytime heating can exceed the overall longwave cooling in the layer, thereby warming the SAL and reenforcing the temperature inversion at its base (Carlson and Benjamin 1980).

Climatologically, the base of the trade wind inversion is less than 500 m off the northwest African coast and rises westward and equatorward to above 2000 m (Hastenrath 1991). In the central tropical North Atlantic, temperature increases through the inversion are generally 1°–2°C. The level at which the SAL mineral dust warms the lower troposphere is approximately coincident with this inversion. Although the dust's effect on microphysical processes is not fully understood, the warming it induces enhances the trade wind inversion, which can limit vertical motions through the SAL (Carlson and Prospero 1972). This stronger inversion may inhibit the development of convection in weak AEWs, as well as allow the SAL to sustain its thermodynamic properties for thousands of kilometers across the Atlantic basin.

Dry air intrusion into the TC circulation. Though it can promote convection along its western and southern boundary (Chen 1985), the dry SAL air can act to suppress convection by enhancing evaporatively driven downdrafts (Emanuel 1989; Powell 1990). We hypothesize that AEWs simply propagate into the SAL, while the low- to midlevel inflow of TCs advect the SAL's low humidity into the TC circulation. This dry air is also associated with reduced values of convective available potential energy (CAPE), a measure of the stability of the atmosphere. Smaller values of CAPE imply greater atmospheric stability and, therefore, reduced convective activity.

Because of the SAL's limited vertical extent, its dry air can be difficult to quantify using the moisture channels on the GOES and Meteosat second-generation (MSG) satellites. The most effective way to study the SAL's low humidity is by first identifying it with the GOES SAL-tracking imagery and then directing aircraft to make in situ measurements of its thermodynamic structure. The National Oceanic and Atmospheric Administration (NOAA) G-IV hurricane surveillance aircraft dispensing GPS sondes (Aberson and Franklin 1999) is an ideal platform to gather complete kinematic and thermodynamic vertical profiles of the SAL and to provide insight into the processes by which the SAL air affects tropical disturbances.

SAL and non-SAL air masses were inadvertently sampled by GPS sondes during operational G-IV missions around Hurricanes Danielle and Georges of 1998 and Hurricanes Debby and Joyce of 2000. Composite vertical profiles of the relative humidity and mixing ratio were generated using the GOES SAL-tracking imagery to examine these air masses in detail. Only GPS sondes that were clearly in SAL or non-SAL tropical air, as indicated by the GOES SAL-tracking imagery (see, e.g., Fig. 1), were used in the composites (10-hPa vertical bins). Figure 2 shows the composite SAL and non-SAL soundings from these four TCs compared with the climatological mean Jordan vertical profiles (Jordan 1958) of the relative humidity and mixing ratio for the region of the West Indies from July to October. The Jordan sounding has lower relative humidities (~10%) and mixing ratios ($\sim 1.5 \text{ g kg}^{-1}$) in the 600–850-hPa layer than the non-SAL composite vertical profile computed from 24 soundings. By contrast, the composite SAL profile (29 soundings) is significantly (99% level determined from a Student's *t* test) different from both the Jordan mean sounding and the non-SAL composite. In the SAL, relative humidities are 25%–45% lower, and mixing ratios average $2.5\text{--}5.5 \text{ g kg}^{-1}$ less between 600 and 850 hPa. For the Hurricane Danielle case, the SAL-targeted GPS sondes indicate that the SAL appears to have maintained its thermodynamic characteristics (Carlson and Prospero 1972) as it moved $\sim 5000 \text{ km}$ across the North Atlantic to a position $< 500 \text{ km}$ off the southeast U.S. coast. The 29 SAL profiles used to create Fig. 2 suggest that the variability of the moisture in the SAL is relatively low. The standard deviation of the 700-hPa relative humidity was $< 8\%$ for these 29 soundings. This figure also suggests that the tropical Atlantic is characterized by a multiple distribution of environmental moisture soundings that is not well represented by a single climatological sounding (e.g., Jordan 1958). Instead, a moist tropical environment exists that is periodically modified by the passage of dry SAL outbreaks. Also, because there was no means of tracking the SAL until recently, it is likely that the climatology originally compiled by Jordan included both SAL and non-SAL soundings. This suggests that the Jordan mean tropical moisture sounding (July–October) may be substantially drier than the typical non-SAL moist tropical sounding that exists in the North Atlantic during this time of year.

Vertical wind shear induced by the SAL midlevel easterly jet. The southern or southwestern edge of the SAL usually coincides with an easterly wind maximum

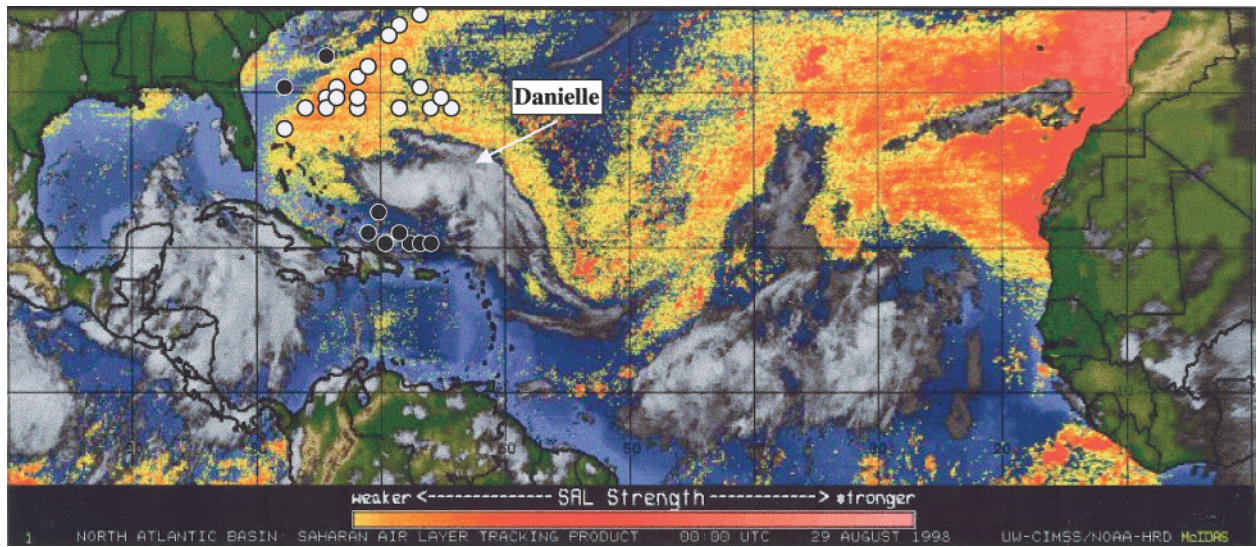


FIG. 1. GOES SAL-tracking satellite imagery with overlaid GPS dropsonde points for Hurricane Danielle on 0000 UTC 29 Aug 1998. The yellow-red shading indicates likely SAL regions with increasing amounts of dust content and dry lower-tropospheric air, as detected by the GOES imagery. Light circles indicate GPS sondes dropped in the SAL environment. Dark circles indicate GPS sondes dropped in non-SAL tropical environments.

near 700 hPa. It is a westward extension of the African easterly jet that is in thermal wind balance with the horizontal temperature gradients that exist between the warm air in the interior of the SAL and cooler tropical air to the south (Carlson and Prospero 1972). The wind speed at the maximum is often 10–17 m s⁻¹ and can be as high as 25 m s⁻¹, which is generally 7–10 m s⁻¹ faster than the typical trade wind

flow. The easterly jet along the SAL's southern boundary can sometimes be tracked using GOES low-level cloud-drift winds and microwave satellite surface winds from QuikSCAT (Liu et al. 1998) and the Special Sensor Microwave Imager (SSM/I; Goodberlet et al. 1989).

GOES SAL-tracking imagery suggests that the SAL's midlevel wind maximum suppresses TC forma-

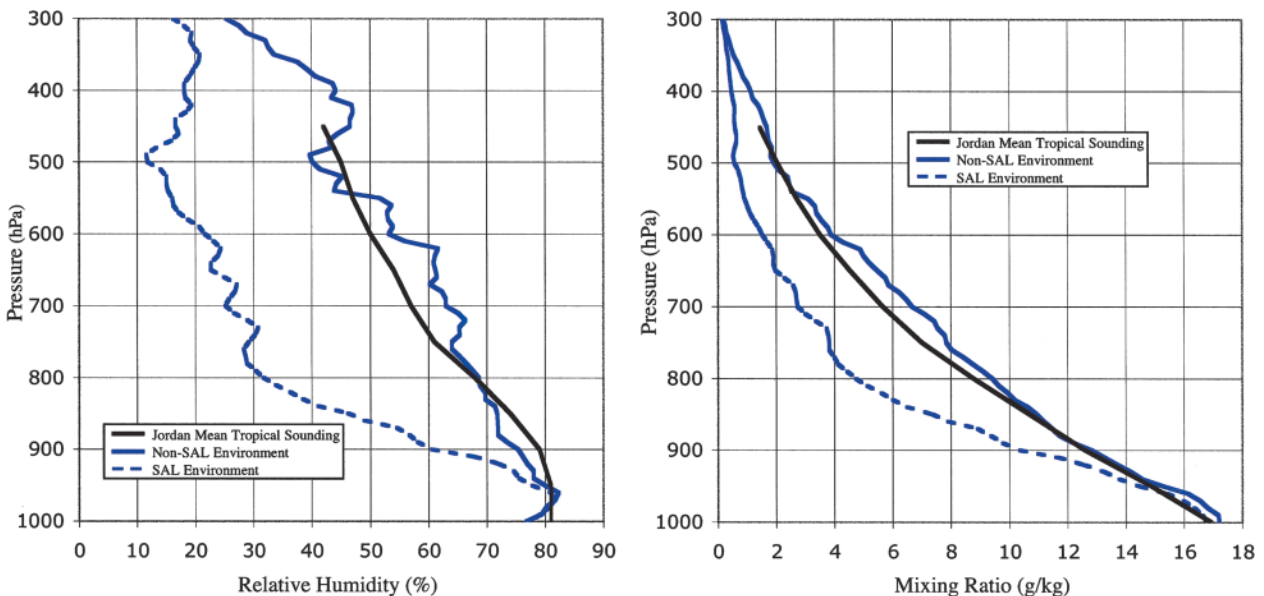


FIG. 2. Composite GPS sonde profiles from sondes launched in the environments of Hurricanes Danielle and Georges of 1998 and Hurricanes Debby and Joyce of 2000. SAL and non-SAL environments were determined using GOES SAL-tracking imagery (see, e.g., Fig. 1). The Jordan mean tropical sounding for the area of the West Indies for Jul-Oct is presented for reference.

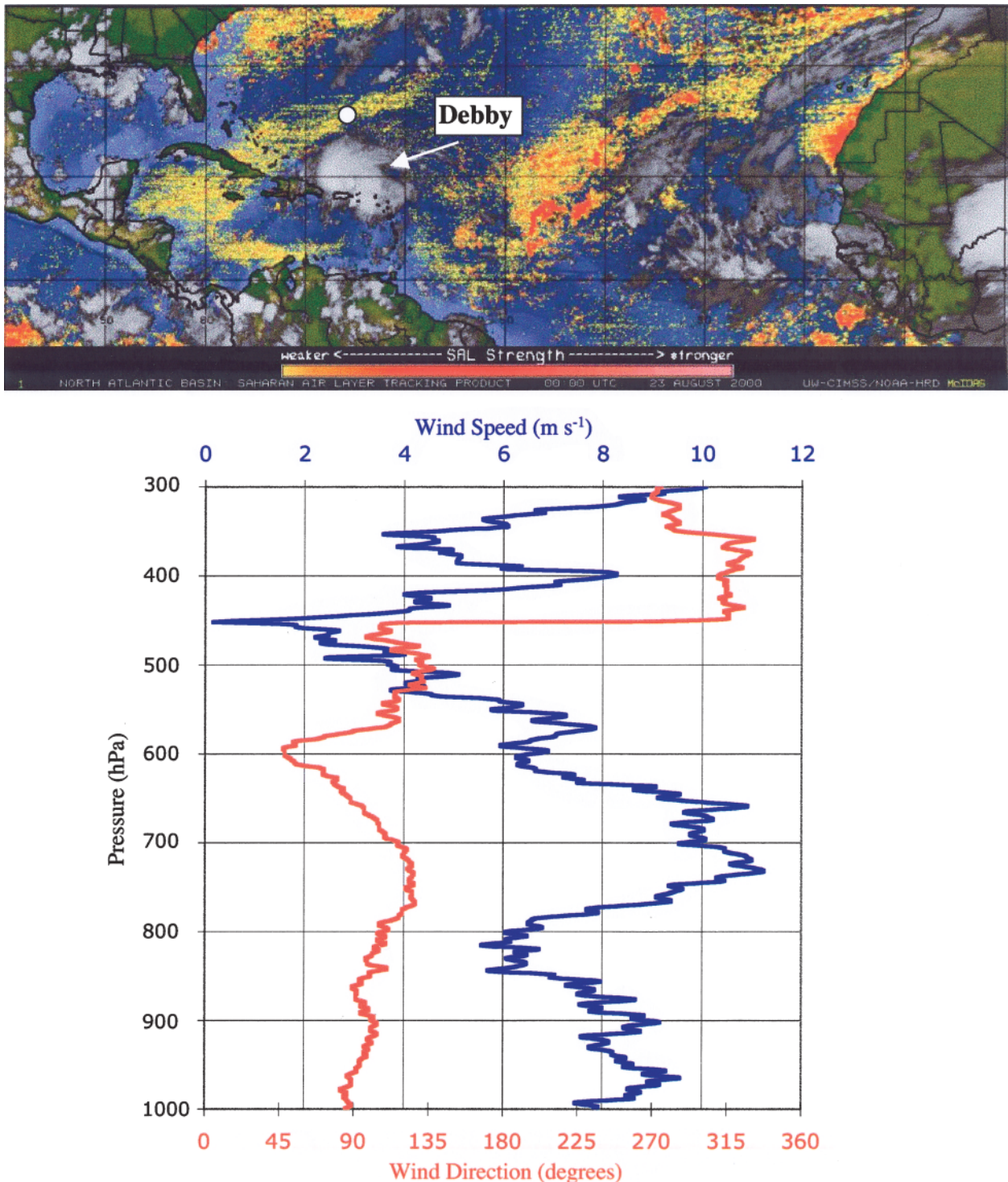


FIG. 3. (top) GOES SAL-tracking satellite imagery with an overlaid GPS dropsonde point ~700 km north-north-east of Hurricane Debby on 0000 UTC 23 Aug 2000. The yellow-red shading indicates likely SAL regions with increasing amounts of dust content and dry lower-tropospheric air, as detected by the GOES imagery. The light circle indicates a GPS sonde dropped in the SAL environment. (bottom) The vertical profiles of wind speed and direction observed by this GPS sonde are plotted.

tion. These embedded strong winds significantly increase the local vertical wind shear by increasing the low- to-midlevel easterly flow. In fact, several of the

TCs examined in this study that were embedded in the SAL (Hurricanes Debby and Joyce of 2000 and Tropical Storm Chantal of 2001) had low-level circu-

lations that raced ahead of their mid- and upper-level deep convection, due to the influence of the SAL's midlevel jet.

The vertical wind shear created by the SAL midlevel jet can be significant, but is often difficult to resolve. First, there is limited lower- and midtropospheric wind data available over the tropical Atlantic. Although GPS index sondes are capable of detecting the strong easterly wind surge often associated with the SAL (see Fig. 3), their use is typically limited spatially and temporally. Second, the SAL's shallow vertical extent (\sim 500–850 hPa) makes it difficult to detect using most remote sensing platforms. For these reasons, the SAL's easterly jet may not be generally well represented in global models. Additionally, typical calculations of the vertical wind shear that use the 850-hPa level to represent the lower-tropospheric winds may produce underestimates in the presence of the SAL. Because the 850-hPa level is usually near the bottom of the SAL (and possibly below it), the true magnitude of the low-to-midlevel winds may be underestimated. The broader 700–925-hPa layer is more useful for representing the wind in the lower troposphere and helps to better resolve the strong vertical wind shear caused by the SAL's low- to midlevel easterly jet.

EFFECTS OF THE SAL ON SPECIFIC ATLANTIC TCS. Hurricane Joyce: September 2000.

Hurricane Joyce formed from an AEW that was positioned several hundred kilometers ahead of a large SAL outbreak. Favorable environmental conditions allowed this AEW to develop from a weak tropical depression late on 25 September 2000 to an 80-kt (41 m s^{-1}) hurricane early on 28 September. The SAL was positioned \sim 500 km northeast of Joyce on 26 September. It overtook Joyce late on 27 September (SAL positioned $< 2^\circ$ from the TC circulation center) and soon began to suppress convection in the storm. Hurricane Isaac (located \sim 1500 km northwest of Joyce at this time) intensified into a category-4 hurricane as it recurved to the northwest and separated from the suppressing influence of the westward-advancing SAL. However, the SAL likely caused Joyce to weaken by imposing low humidity and strong vertical wind shear on the main circulation.¹ During the next 48 h, Joyce weakened to a moderate tropical storm, and

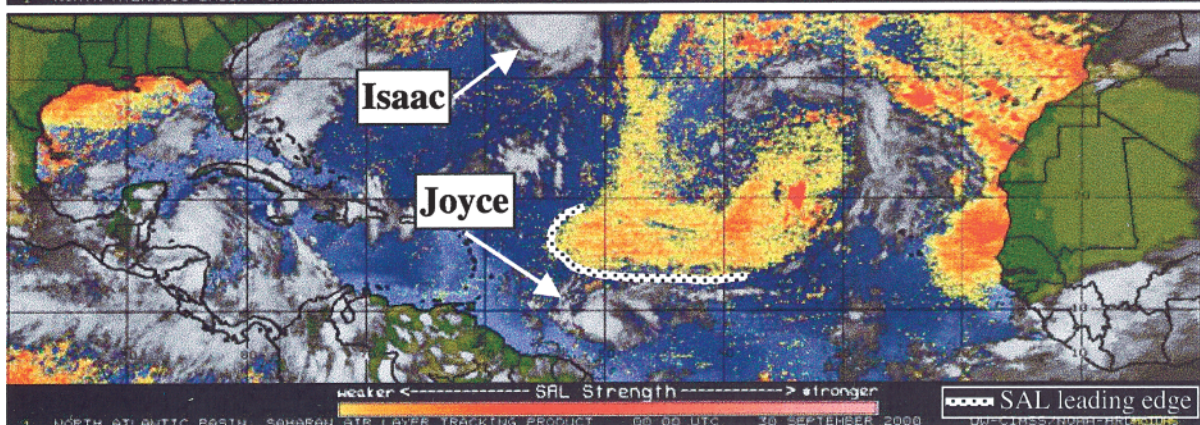
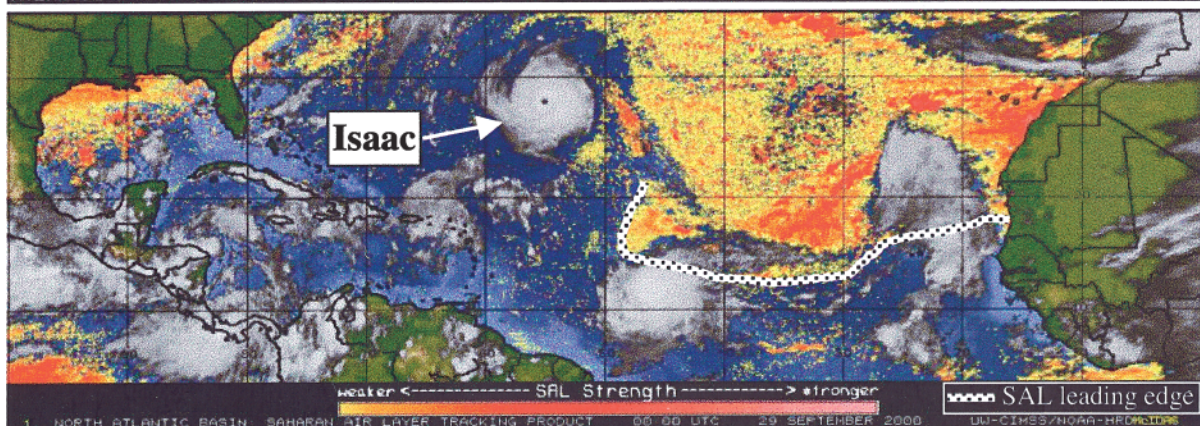
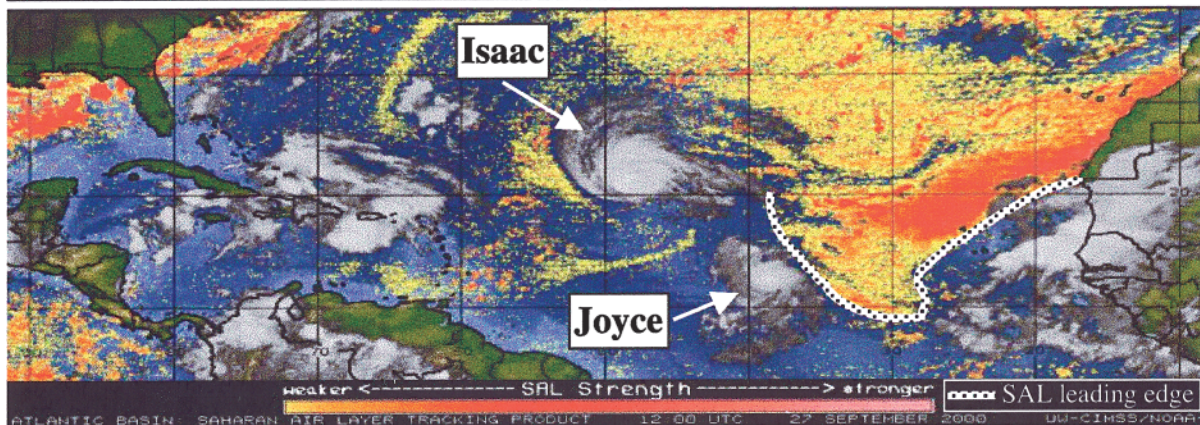
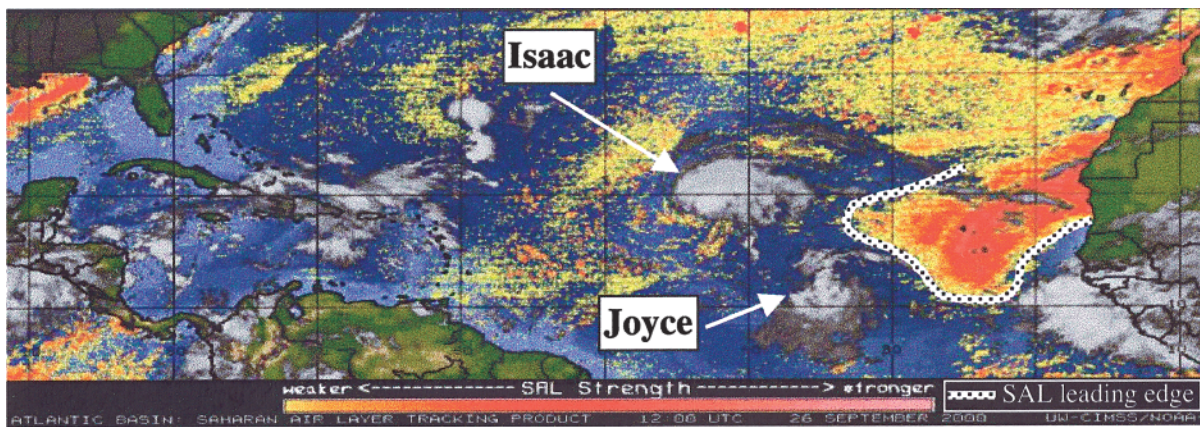
within 96 h it became a disorganized tropical depression. The sequence described above is illustrated in Fig. 4's time series depiction of Joyce, Isaac, and the SAL from 26 to 30 September, and in Fig. 5's best-track intensity plot for Joyce.

Early on 28 September marked the beginning of Joyce's weakening trend. Prior to this, the Statistical Hurricane Intensity Prediction Scheme (SHIPS; DeMaria and Kaplan 1999) had been underforecasting the 24- and 48-h intensities for Joyce (Fig. 5). Figure 5 indicates that after the SAL reached Joyce, the SHIPS 24- and 48-h intensity forecasts were overestimated by as much as \sim 40–55 kt (\sim 20–28 m s^{-1}), likely due to increased vertical wind shear and dry air entrainment, which were not effectively represented by the model data used in the SHIPS scheme. GOES-8 low-level (600–925 hPa) cloud-drift winds indicated that the SAL wind-surge strength was $10\text{--}18 \text{ m s}^{-1}$ just northeast of Joyce. Consequently, the vertical wind shear northeast of Joyce increased to 40–60 kt ($20\text{--}30 \text{ m s}^{-1}$) by 0000 UTC on 28 September (Fig. 6). The University of Wisconsin—Madison (UW) Cooperative Institute for Meteorological Satellite Studies (CIMSS) wind shear calculation shown in Fig. 6 is calculated by differencing the winds in the 150–350-hPa and 700–925-hPa layers using data from the U.S. Navy Operational Global Atmospheric Prediction System (NOGAPS) model and GOES water vapor and cloud-drift satellite winds. This algorithm removes the circulation associated with the TC vortex from the grid field and uses bilinear interpolation to replace the vortex region with environmental values that surround the storm.

The UW CIMSS vortex extraction procedure may produce underestimates of vertical wind shear in cases like Hurricane Joyce, where the northeast SAL quadrant of the storm contains high wind shear (40–60 kt, $20\text{--}30 \text{ m s}^{-1}$) and the other non-SAL quadrants have much lower values of wind shear (0–10 kt, 0–5 m s^{-1}). SHIPS calculates vertical wind shear by averaging the shear values in the 200–800-km radius around the TC. This technique will also tend to underestimate the

FIG. 4. (facing page) GOES SAL-tracking satellite imagery time series showing Hurricane Joyce's interaction with the SAL (top) 1200 UTC 26 Sep 2000, (middle top) 1200 UTC 27 Sep 2000, (middle bottom) 0000 UTC 29 Sep 2000, and (bottom) 0000 UTC 30 Sep 2000. The yellow-red shading indicates likely SAL regions and increasing amounts of dust content and dry lower-tropospheric air, as detected by the GOES imagery. The dotted lines indicate the western and southern boundaries of the advancing SAL.

¹ Although it is uncertain exactly how long it will take the SAL's dry air and enhanced vertical wind shear to weaken a TC, the time delay and extent of weakening are likely proportional to the size and strength of the TC's circulation. This aspect of the SAL requires further research.



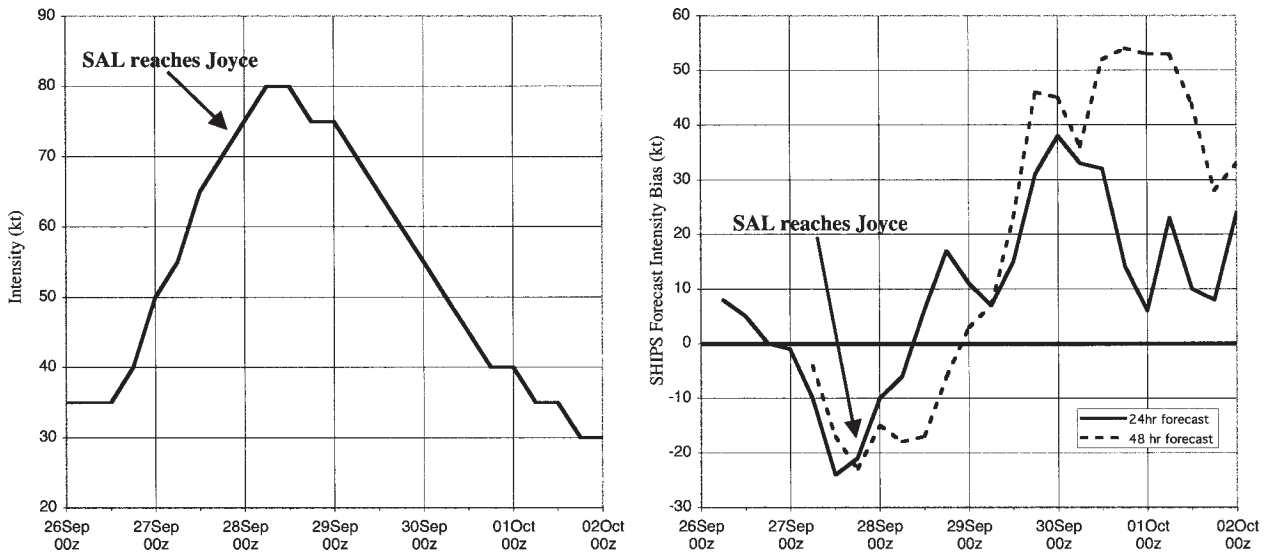


FIG. 5. (left) Hurricane Joyce best-track intensity and (right) SHIPS forecast intensity bias for the period from 26 Sep to 2 Oct 2000. The approximate time at which the SAL overtook the storm is indicated in both plots.

wind shear in cases such as Hurricane Joyce when the shear magnitude is asymmetrically distributed around the TC. Therefore, the vertical wind shear at Hurricane Joyce's location may have been higher than is being depicted for 0000 UTC 28 September by the UW CIMSS shear analysis (Fig. 6) and by SHIPS (16 kt , 8 m s^{-1}).

The presence of the SAL was also confirmed by a NOAA G-IV surveillance flight on 30 September.

GPS sondes launched during this flight detected SAL air with relative humidities as low as 5% and mixing ratios as low as 1 g kg^{-1} in the 600–850-hPa layer 400–500 km north and west of Joyce.

1999–2002 Atlantic TCs. The best-track intensities for several 1999–2001 Atlantic TCs that interacted with SAL are shown in Fig. 7. GOES SAL-tracking imagery was used to determine if a TC's circulation center was in proximity ($< 2^\circ$) to the SAL. Figure 8 is similar to Fig. 7 and shows the 24- and 48-h bias of the SHIPS intensity forecasts relative to National Hurricane Center best-track intensities.

Hurricanes Cindy and Floyd of 1999 and Erin and Felix of 2001 represent TCs that were initially under the influence of the SAL (Fig. 7). All of these TCs eventually emerged from the SAL and attained major hurricane status. This scenario is depicted for Hurricane Erin in Fig. 9. Erin immediately began interacting with the SAL as it emerged from the North African coast. It became embedded in the SAL and struggled to maintain tropical storm intensity for the next several days. However, when Erin emerged from the SAL as a 35-kt (18 m s^{-1})

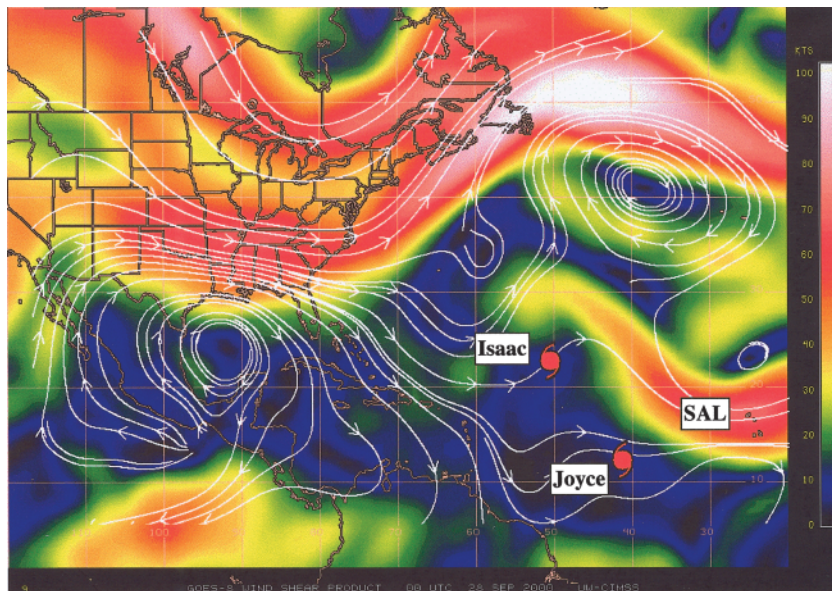


FIG. 6. Vertical wind shear (kt) for 0000 UTC 28 Sep 2000. Shear values are indicated by colored shading and were calculated by differencing the mean wind vectors of the 150–350- and 700–925-hPa layers. The shear vector is indicated by the white streamlines. Hurricanes Joyce and Isaac, as well as the strong vertical shear induced by the SAL, are indicated.

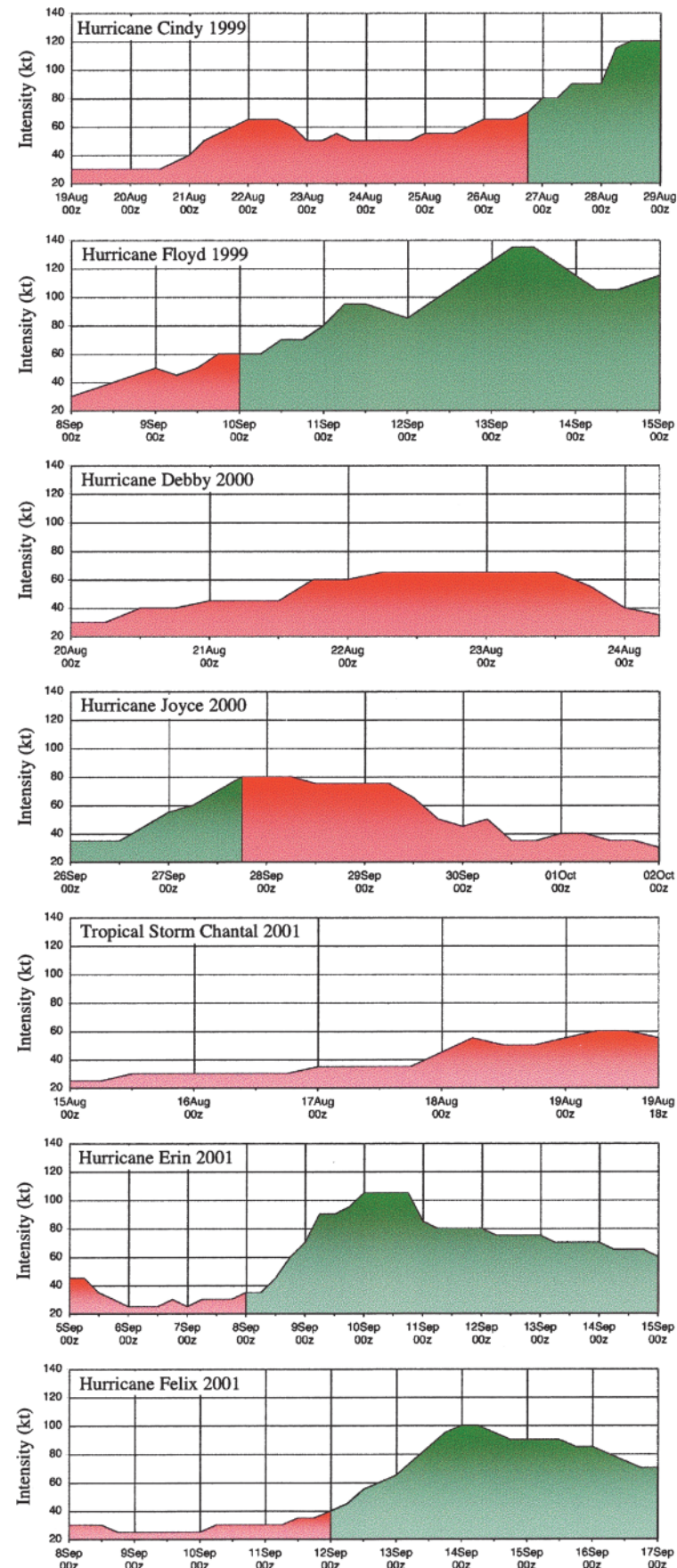
tropical storm at 0000 UTC 8 September, it rapidly intensified into a 105-kt (54 m s^{-1}) major hurricane within just 48 h (Fig. 7).² SHIPS overforecast Erin's intensity (up to 45 kt, 23 m s^{-1}) while it was in the SAL and underforecast its intensity (up to 50 kt, 26 m s^{-1}) as it began to emerge from the SAL (Fig. 8).

Hurricane Debby of 2000 and Tropical Storm Chantal of 2001 were never able to separate from the SAL. These systems struggled to maintain their intensities and were consistently overforecast by SHIPS (Figs. 7 and 8). Tropical Depression No. 7 of 2002 (not shown) was overrun by the SAL. This 30-kt (15.5 m s^{-1}) TC dissipated into a disorganized area of convection less than 24 h after the SAL engulfed it early on 8 September.

Figure 7 demonstrates the suppressing influence of the SAL on TC activity and indicates that TCs that are being affected by the SAL tend to weaken or have difficulty intensifying into mature hurricanes. Figure 8 indicates that SHIPS has difficulty predicting the intensities of TCs transitioning into or out of the SAL and tends to overestimate intensity forecasts of TCs that are interacting with the SAL.

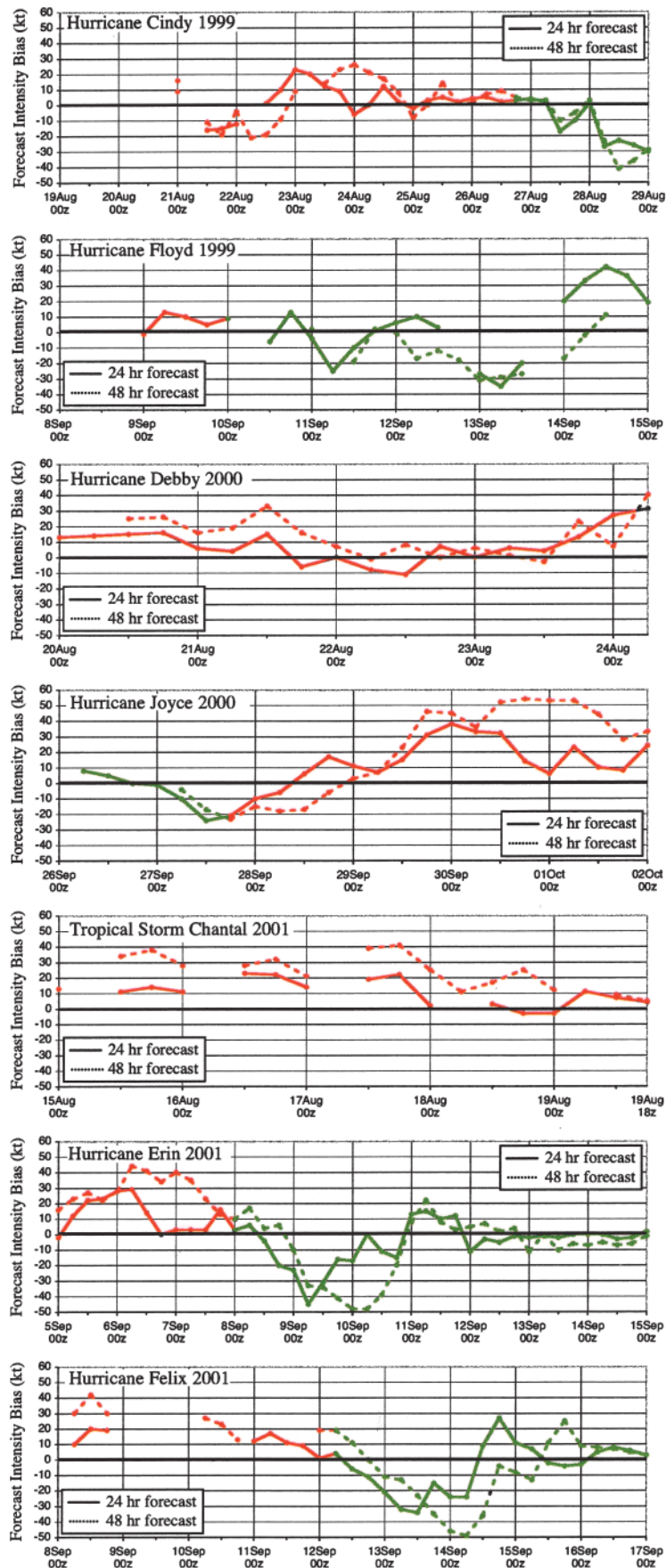
SUMMARY AND CONCLUSIONS.

The GOES multispectral technique described here creates a unique kind of satellite image that allows tracking of the SAL across the North Atlantic basin and



² The satellite imagery begins to detect what is likely polluted continental air north of Erin on 8 September (Fig. 9). This air mass is unrelated to the SAL air that is positioned south of Erin from the central Caribbean to the west coast of Africa and appears not to have significantly affected Erin's intensity.

FIG. 7. Time series of NHC best-track intensity for several Atlantic tropical cyclones in 1999 through 2001. Red shading indicates that the TC was under the suppressing influence of the SAL. Green shading indicates periods when the SAL was not impacting the TC.



has provided some insight into the relationship between the SAL and North Atlantic TCs. The satellite imagery also reveals that the size of the SAL over the Atlantic, usually in the region of 15°–30°N, can exceed an area larger than the contiguous United States. Of more significance, the SAL appears to affect TC intensity change in the North Atlantic. It suppresses the intensity of TCs that it engulfs (Joyce 2000), while TCs that emerge from its influence (Erin 2001) can rapidly develop into strong hurricanes.

The GOES SAL-tracking satellite imagery also suggests that a possible link exists between the SAL and the overall TC activity that occurs in the North Atlantic. The North Atlantic basin averages about 10 named TCs per year. This represents ~40% and ~60% less annual TC activity than typically occurs in the eastern North Pacific (16.5 named storms) and western North Pacific (26 named storms) basins, respectively (Neumann 1993). There are climatological differences between Atlantic and Pacific basins that may account for some of the variation in TC activity between these ocean basins. However, the presence of the SAL and its ability to inhibit the growth of the North Atlantic's large number of seedlings (AEWs; Pasch et al. 1998) into named TCs may be a factor contributing to the relatively smaller number of TCs that typically occur in this basin each year. Several conclusions and recommendations can be drawn from this study:

- The SAL appears to suppress Atlantic TC activity in three main ways. First, it introduces dry, stable air into the storm, which promotes convectively driven downdrafts in the TC. Second, the SAL's midlevel easterly jet can dra-

FIG. 8. Time series of the SHIPS 24- and 48-h intensity bias relative to the NHC best track for the several Atlantic tropical cyclones shown in Fig. 7. Red lines indicate that the TC was under the suppressing influence of the SAL. Green lines indicate periods when the SAL was not impacting the TC.

matically enhance the local vertical wind shear. Third, the SAL enhances the preexisting trade wind inversion in the Atlantic, which acts to stabilize the environment.

- The extremely dry air that characterizes the SAL appears to undergo surprisingly little modification as it traverses the North Atlantic. The temperature inversion typically found at the SAL's base may contribute to the longevity of this dry air.
- The tropical North Atlantic is likely characterized by a multiple distribution of environmental moisture soundings that include moist tropical and SAL. This suggests that the mean Jordan tropical sounding (July–October) may be substantially drier than the typical non-SAL moist tropical soundings that exists in the North Atlantic during this time of year.
- Data from GPS sondes (that have inadvertently sampled the SAL) and GOES satellite-derived

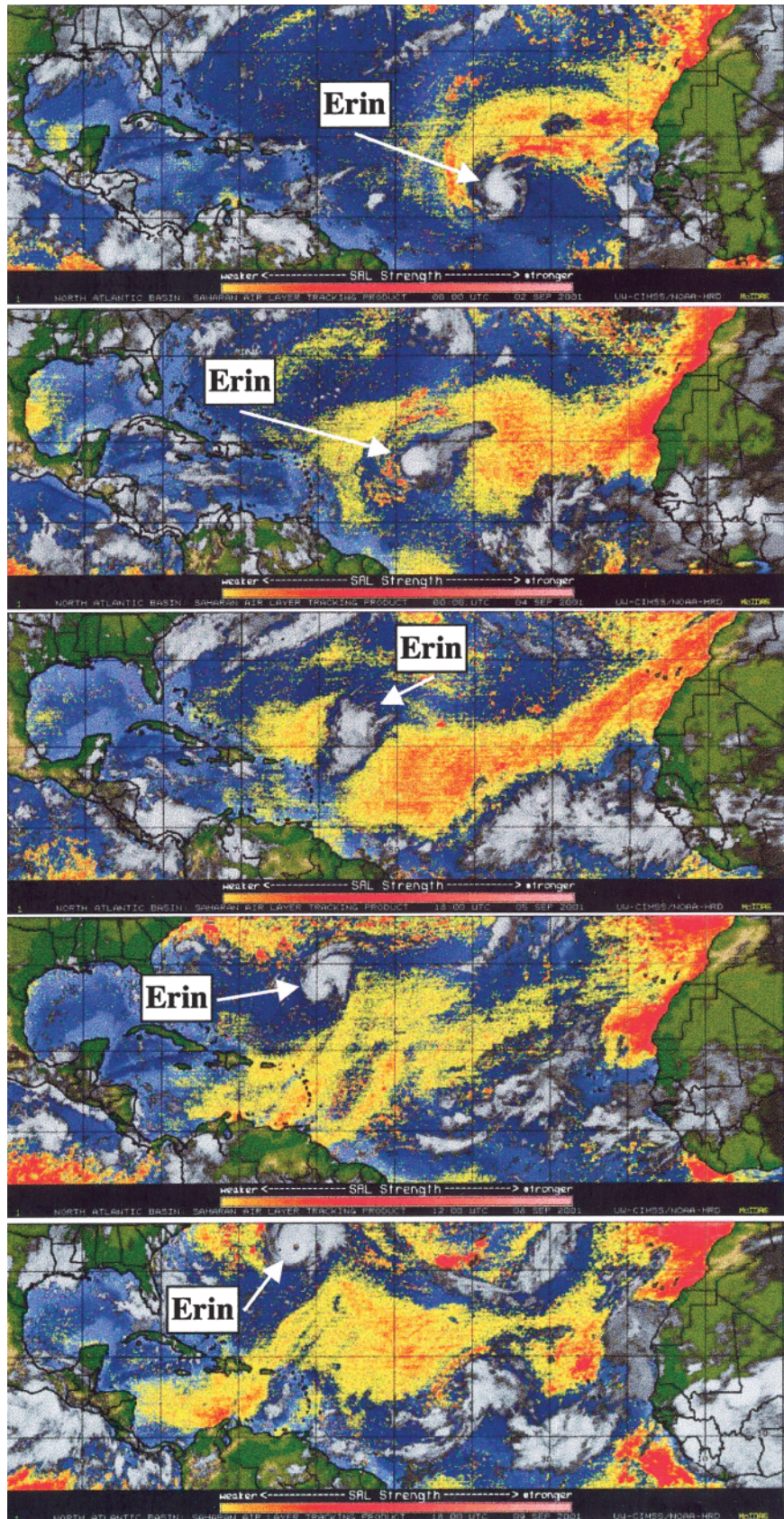


FIG. 9. GOES SAL-tracking imagery time series showing Hurricane Erin's interaction with the SAL at (top to bottom) 0000 UTC 2 Sep 2001, 0000 UTC 4 Sep 2001, 1800 UTC 5 Sep 2001, 1200 UTC 8 Sep 2001, and 1800 UTC 9 Sep 2001. The yellow-red shading indicates likely SAL regions with increasing amounts of dust content and dry lower-tropospheric air, as detected by the GOES imagery.

winds suggest the importance of assimilating the SAL-induced vertical wind shear and moisture information into forecast models.

- The intensity change of TCs influenced by the SAL may not be well predicted by the operational SHIPS model. SHIPS does not specifically consider the SAL in its methodology and relies on model data that may not effectively represent the SAL's thermodynamic properties.
- The presence of SAL signatures in the GOES SAL-tracking satellite imagery shows promise as a predictor for both TC nonintensification as well as rapid deepening.

Future work regarding the SAL will involve further validation of the GOES SAL-tracking imagery using GPS sondes. A more detailed understanding of SAL-TC interactions can be attained utilizing U.S. Air Force Reserve Command and NOAA aircraft that are able to collect measurements of the lower troposphere. This effort could be supplemented by improved SAL detection that uses high-resolution satellite imagery, such as the Moderate Resolution Imaging Spectroradiometer (MODIS) on the *Terra* and *Aqua* satellites, and total precipitable water estimates from the constellation of SSM/I satellites. This wide array of observations could also be used to assess how effectively forecast models capture the SAL's thermodynamics and how this information could be optimally utilized to improve model forecasts.

ACKNOWLEDGMENTS. This study was the result of collaborative efforts between the NOAA/AOML/Hurricane Research Division and the UW CIMSS. The authors would like to thank Dr. Robert Burpee for his insight and meticulous reviews of the various versions of this manuscript. Thanks to John Kaplan of HRD for his input into this work as it related to the SHIPS intensity forecast model, as well as Dr. Frank Marks of NOAA/HRD and Dr. Joseph Prospero of the University of Miami CIMAS for their insightful input and general knowledge of the Saharan air layer. Special thanks also to David Stettner of UW CIMSS for his assistance in retrieving the vast amount of archived GOES satellite imagery and UW CIMSS cloud-drift wind and wind shear data that were instrumental in carrying out this work. This paper benefited from reviews by Dr. Robert Burpee of the University of Miami CIMAS, Dr. Christopher Landsea and Dr. Frank Marks of NOAA/HRD, and Dr. Hugh Willoughby of Florida International University.

REFERENCES

- Aberson, S. D., and J. L. Franklin, 1999: Impact on hurricane track and intensity forecasts of GPS dropwindsonde observations from the first-season flights of the NOAA Gulfstream-IV jet aircraft. *Bull. Amer. Meteor. Soc.*, **80**, 421–427.
- Burpee, R. W., 1972: The origin and structure of easterly waves in the lower troposphere of North Africa. *J. Atmos. Sci.*, **29**, 77–90.
- Carlson, T. N., and J. M. Prospero, 1972: The large-scale movement of Saharan air outbreaks over the northern equatorial Atlantic. *J. Appl. Meteor.*, **11**, 283–297.
- , and S. G. Benjamin, 1980: Radiative heating rates of Saharan dust. *J. Atmos. Sci.*, **37**, 193–213.
- Chen, Y.-L., 1985: Tropical squall lines over the eastern Atlantic during GATE. *Mon. Wea. Rev.*, **113**, 2015–2022.
- DeMaria, M., and J. Kaplan, 1999: An updated Statistical Hurricane Intensity Prediction Scheme (SHIPS) for the Atlantic and eastern North Pacific basins. *Wea. Forecasting*, **14**, 326–337.
- Diaz, H. F., T. N. Carlson, and J. M. Prospero, 1976: A study of the structure and dynamics of the Saharan air layer over the northern equatorial Atlantic during BOMEX. National Hurricane and Experimental Meteorology Laboratory NOAA Tech. Memo. ERL WMPO-32, 61 pp.
- Emanuel, K. A., 1989: The finite-amplitude nature of tropical cyclogenesis. *J. Atmos. Sci.*, **46**, 3431–3456.
- Goldenberg, S. B., and L. J. Shapiro, 1996: Physical mechanisms for the association of El Niño and West African rainfall with Atlantic major hurricane activity. *J. Climate*, **9**, 1169–1187.
- Goodberlet, M. A., C. T. Swift, and J. C. Wilkerson, 1989: Remote sensing of ocean surface winds with the Special Sensor Microwave/Imager. *J. Geophys. Res.*, **94**, 14 547–14 555.
- Hastenrath, S., 1991: *Climate Dynamics of the Tropics*. Kluwer Academic, 488 pp.
- Hock, T. F., and J. L. Franklin, 1999: The NCAR GPS dropwindsonde. *Bull. Amer. Meteor. Soc.*, **80**, 407–420.
- Jordan, C. L., 1958: Mean soundings for the West Indies area. *J. Meteor.*, **15**, 91–97.
- Karyampudi, V. M., and T. N. Carlson, 1988: Analysis and numerical simulations of the Saharan air layer and its effect on easterly wave disturbances. *J. Atmos. Sci.*, **45**, 3102–3136.
- Liu, W. T., W. Tang, and P. S. Polito, 1998: NASA scatterometer provides global ocean surface wind

- fields with more structures than numerical weather prediction. *Geophys. Res. Lett.*, **25**, 761–764.
- Neumann, C. J., 1993: Global overview. Global Guide to Tropical Cyclone Forecasting, World Meteorological Organization Tech. Rep. WMO/TC 560, Rep. TCP-31.
- Pasch, R. J., L. A. Avila, and J. Jing, 1998: Atlantic tropical systems of 1994 and 1995: A comparison of a quiet season to a near-record-breaking one. *Mon. Wea. Rev.*, **126**, 1106–1123.
- Powell, M. D., 1990: Boundary layer structure and dynamics in outer hurricane rainbands. Part II: Downdraft modification and mixed-layer recovery. *Mon. Wea. Rev.*, **118**, 918–938.
- Prata, A. J., 1989: Observations of volcanic ash clouds in the 10–12 micrometer window using AVHRR/2 data. *J. Remote Sens.*, **10**, 751–761.
- Prospero, J. M., and T. N. Carlson, 1972: Vertical and areal distributions of Saharan dust over the western equatorial North Atlantic Ocean. *J. Geophys. Res.*, **77**, 5255–5265.
- Velden, C. S., T. L. Olander, and S. W. Wanzong, 1998: The impact of multispectral GOES-8 wind information on Atlantic tropical cyclone track forecasts in 1995. Part I: Dataset, methodology, description, and case analysis. *Mon. Wea. Rev.*, **126**, 1202–1218.